Effects of Rate-Shaped and Multiple Injection Strategies on Pollutant Emissions, Combustion Noise and Fuel Consumption in a Low Compression Ratio Diesel Engine

EFFECTS OF RATE-SHAPED AND MULTIPLE INJECTION STRATEGIES ON POLLUTANT EMISSIONS, COMBUSTION NOISE AND FUEL CONSUMPTION IN A LOW COMPRESSION RATIO DIESEL ENGINE

Stefano d'Ambrosio *, Alessandro Ferrari, Alessandro Mancarella and Antonio Mittica

Energy Department, Politecnico di Torino, Corso Duca degli Abruzzi 24, 10129, Italy

(*Received date ; Revised date ; Accepted date*) * Please leave blank

ABSTRACT – An experimental investigation has been carried out to highlight the effects of different injection strategies on the performance and emissions of a low compression ratio Euro 5 diesel engine operated with high EGR rates. Rate-shaped main injections, achieved with piezoelectric and solenoid injectors by means of boot and injection fusion, respectively, as well as optimized multiple injection patterns have been compared. The results of the comparisons, performed with reference to a state-of-the-art double pilot-Main (*pM*) strategy, are presented in terms of engine-out exhaust emissions, combustion noise (CN) and fuel consumption.
Rate-shaped main injections, when included in delayed multiple injection patterns, have shown a minor influence on reducing NO_x, while a slight deterioration in soot has been found. Both a double pilot and a boot injection schedule have been able to reduce CN at low loads. A higher reduction in CN has been obtained with an injection fusion event. Finally, DoE optimized triple and quadruple injection strategies have led to improved soot-NO_x trade-offs, with respect to the *pM* calibration. In fact, splitting the injection helps to entrain air inside the fuel plumes, thus creating locally leaner mixture (less prone to forming soot) and allowing increasing the EGR rates (reducing NO_x formation).

KEY WORDS : multiple injections; rate-shaped injection; boot injection; closely-coupled injections; DoE calibration optimization

NOMENCLATURE

aTDC : after top dead center
bM : rate-shaped (boot) main injection (obtained with DAP injectors)
bMa : rate-shaped (boot) main and after injection strategy (obtained with DAP injectors)
bmep : brake mean effective pressure
bsfc : brake specific fuel consumption
bTDC : before top dead center
CA : crank angle (degree)
CN : combustion noise
DAP : direct acting piezoelectric
DOC : diesel oxidation catalyst
DoE : design of experiment
DPF : diesel particulate filter
DT : dwell time
ECU : electronic control unit
EGR : exhaust gas recirculation
HC : unburned hydrocarbons
HRR : heat release rate
IAP : indirect acting piezoelectric
IAS : indirect acting solenoid
ID : ignition delay
imep : indicated mean effective pressure
LTC : low temperature combustion
m : mass
MFB50 : angle at which 50% of the combustion mixture has burned
n : engine speed
NEDC : new European driving cycle
NO_x : nitrogen oxides
OEM : original equipment manufacturer
p : pressure
pbM : pilot and rate-shaped (boot) main injection strategy (obtained with DAP injectors)
pbMa : pilot, rate-shaped (boot) main and after injection strategy (obtained with DAP injectors)
PCCI : premixed charge compression ignition
PM : particulate matter
pM : pilot and main injection strategy
pMa : pilot, main and after injection strategy

* *Corresponding author*. stefano.dambrosio@polito.it

pmM : pilot and rate-shaped main injection strategy (with injection fusion)
ppM : double pilot and main injection strategy
ppMa : double pilot, main and after injection strategy
q : fuel injected quantity
SOC : start of combustion
SOI : electrical start of injection
T : Temperature
T_{CHA} : charging time of the DAP injector needle
TDC : top dead center
T_{exh} : exhaust gas temperatures
T_{HLD} : holding time of the DAP injector needle
X_{EGR} : mass fraction of exhaust gas recirculation
ϕ : equivalence ratio

SUBSCRIPTS

Aft : after injection
b : burned gas
Boot : boot injection
exh : exhaust gas
int : intake gas
Main : main injection
max : maximum value
Pil,1 : closer to the main pilot injection
Pil,2 : further from the main pilot injection
Rail : fuel common rail

1. INTRODUCTION

In the recent years, diesel engines have been used extensively in both passenger cars and in the heavy-duty sector, especially in Europe. These engines feature a higher fuel conversion efficiency than their gasoline counterparts, and they represent a viable solution to meet the new CO_2 emission reduction targets. However, their higher nitrogen oxide (NO_x) and particulate matter (PM) emissions partially counterbalance the benefits [Balaji *et al.*, 2013; Heywood, 2018], although great progress has been made in recent years to improve both the in-cylinder combustion [Fang *et al.*, 2012; Finesso *et al.*, 2019] and after-treatment systems [Reşitoğlu *et al.*, 2014]. As far as technologies aimed at limiting in-cylinder pollutant emissions are concerned, non-conventional diesel combustion concepts and fuel injection strategies play fundamental roles.

Among the various new combustion concepts, the so-called Premixed Charge Compression Ignition (PCCI), which belongs to the more general Low Temperature Combustion (LTC) class, is perhaps one of the most promising at low and medium loads, as it allows a simultaneous reduction of both NO_x and PM emissions [Catania *et al.*, 2009, 2010; Kook *et al.*, 2005]. NO_x can be limited by using a large amount of exhaust gas recirculation (EGR), in order to lower the in-cylinder combustion peak temperatures [Maiboom *et al.*, 2008], while PM formation can be contained by enhancing the premixed combustion phase and thus hindering the creation of locally rich fuel pockets at the start of combustion (SOC) [O'Connor and Musculus, 2014b]. This premixed charge can be obtained by either advancing the start of injection (SOI) well before the top dead center (TDC), or by using a delayed SOI, with respect to the values adopted for the conventional combustion mode. In the former case, which is referred to as early PCCI strategy, the injection pattern is shifted early during the compression stroke into a charge with relatively low density, and a high EGR rate is implemented, thus prolonging the fuel ignition delay (ID). In this way, the combustion mainly develops in the premixed stage, and gives rise to high in-cylinder pressure derivatives and combustion noise (CN), which limits the implementation of this strategy only to low engine loads. In the latter case, which is referred to as late PCCI strategy, the injection pattern is instead delayed in proximity of the TDC, allowing the combustion to mainly develop during the expansion stroke, with ensuing penalties in terms of engine efficiency [Musculus *et al.*, 2013], but with fewer constraints on CN, which can even improve at low loads.

As far as fuel injection strategies are concerned, the development of modern Common Rail fuel injection systems [Catania *et al.* 2006, Mittica *et al.* 2004], equipped with advanced diesel injectors that are able to manage very small fuel injection quantities [Ferrari *et al.*, 2012, 2016, 2018a] at very high pressure levels and with reduced injector leakage [Ferrari *et al.*, 2018b], has paved the way toward the implementation of advanced injection strategies in diesel engines [Ferrari and Mittica, 2016]. Flexible multiple injection and rate-shaping events are some of the possible feasible solutions [Ferrari and Mittica, 2012].

Pilot and after injections are the two fundamental ways of splitting a main injection shot into separate injection events, and both of them can be implemented in the same engine cycle. Moreover, the main injections can be rate-shaped realizing rectangular, ramp or boot injection strategies, which may be achieved by means of direct acting piezoelectric (DAP) [Ferrari and Mittica, 2012] or hydraulically amplified injectors. When DAP injectors are used to obtain boot profiles, the injector needle has to be kept at part lift during the boot phase and, as an additional current charge is given to the piezo-stack, the needle reaches its stroke-end and the fuel mass flowrate reaches its maximum value [Ferrari et al., 2012, 2016; Ferrari and Mittica, 2012]. Distinctive results can also be achieved by adopting latest generation solenoid injectors and decreasing the dwell time (DT) between the pilot and the following main shot to very short durations. In this way, injection fusion phenomena and fuel-rate shaped

profiles similar to those achievable by means of DAP injectors are obtained.

The combustion of a pilot injection slightly raises the in-cylinder pressure and temperature conditions before the main injection event [Heywood, 2018; Maiboom *et al.*, 2008]. This in turn shortens the ID of the main injected fuel, which develops more in the mixing-controlled phase, but with a lower peak temperature value in correspondence to the diffusive flames, generally leading to a reduced NO_x production [Maiboom *et al.*, 2008; d'Ambrosio and Ferrari, 2015b]. If larger pilot injection quantities are implemented, the pilot combustion shows sharper rises in the in-cylinder gas temperature than in the case of smaller shots, increasing their own NO_x production levels and possibly outmatching the subsequent decrease in NO_x produced during the main combustion [Okude *et al.*, 2007; d'Ambrosio and Ferrari, 2016]. NO_x emissions can also be influenced by rate-shaped main injections. For instance, an initial boot phase during the main injection influences both the fuel atomization/mixing processes and the heat release rate, because the reduced injection pressure and the lower fuel mass flow-rate during the boot phase affect the balance between the premixed and diffusive combustion stages [Desantes *et al.*, 2004b].

A pilot injection that is closely-coupled to the main shot generally increases soot production. As the fuel spray of the main shot is injected, it can encounter burned pilot combustion gases, which have created a hotter environment that lacks oxygen. The higher temperature reduces the fuel lift-off length during the main injection and the consequent air entrainment in the spray, and this leads to higher equivalence ratios close to the nozzle and higher soot formation [Helmantel and Golovitchev, 2009]. A similar detrimental effect on soot production is usually reported for boot injections [Desantes *et al.*, 2004a, 2004b]. In this context, the introduction of an after-injection at the end of the main injection could be useful to enhance the oxidation of the previously produced soot particles [Desantes *et al.*, 2007; d'Ambrosio and Ferrari, 2015c]. A small after shot may be exploited to reduce the temporal length of the main injection: the main rich core develops under leaner equivalence ratios as the fuel injection is interrupted for a short time between the two shots [d'Ambrosio and Ferrari, 2015a]. Moreover, an after injection can provide additional thermal energy during the expansion stroke which may further oxidize all the carbonaceous species, including soot particles [d'Ambrosio *et al.*, 2018].

The behavior of *bsfc,* when multiple injection schedules are adopted, depends on the timing and fuel quantity of each shot. The fuel consumption becomes worse as either the pilot injection timing advances or the pilot injected fuel quantity increases [Ehleskog *et al.*, 2007]. Similarly, if the after injection timing is too far from the main combustion, *bsfc* tends to undergo penalties because the late injected fuel promotes wall wetting and rapidly makes HC emissions increase [d'Ambrosio and Ferrari, 2015c; Hoimyung *et al.*, 2013]. Nevertheless, when boot injection strategies are applied, *bsfc* generally increases, especially for higher engine loads, due to the extended combustion duration [Desantes *et al.*, 2004a].

Finally, both pilot and boot injection strategies can be effective in reducing CN, with major benefits for lower engine loads [d'Ambrosio and Ferrari, 2015c, 2016]. The implementation of a boot injection phase under high rail pressures can further reduce CN, compared to a pilot-main injection schedule [Kastner *et al.*, 2009].

The potentialities of several fuel injection patterns, featuring multiple shots and rate-shaping, have been explored in the present paper. Design of experiment (DoE) techniques have been used to obtain optimal calibrations for the multiple injection strategies, except for the pilot-main injection schedule, which represented a state-of-the-art calibration. The results, in terms of exhaust pollutant emissions, fuel consumption and CN, have been measured under different steady-state engine working conditions characterized by the presence of high EGR rates. The objective has been to assess whether injection rate shaping, coupled with split injection strategies featuring pilot and/or after shots, can introduce any benefits to efficient multiple injection strategies.

2. EXPERIMENTAL FACILITIES AND ENGINE SETUP

The investigation dealt with in the present work has been conducted on a 2.0 liter, four-cylinder, four-stroke diesel engine (whose main features are reported in Table 1) manufactured by General Motors and fueled with conventional diesel oil. It is homologated for Euro 5 regulations and equipped with a twin-stage turbocharger regulated by valve actuators and wastegate valves, a high-pressure common-rail injection system and a short-route cooled EGR circuit. It was originally provided by

Table 1: Main specifications of the test engine

Engine type	2.0 l diesel Euro 5
Displacement [cm^3]	1956
Bore [mm] × stroke [mm]	83.0 × 90.4
Compression ratio	16.3
Valves per cylinder	4
Turbo	Twin-stage, wastegate valves
Fuel injection system	Common Rail 2000 bar
EGR system	Short-route cooled EGR
Specific power [kW/l]	71
Specific torque [Nm/l]	205

the OEM with indirect-acting piezoelectric (IAP) injectors and it was then tested with direct-acting piezoelectric (DAP) and new-generation indirect-acting solenoid (IAS) injectors to perform advanced injection strategies, that is, boot and closely-coupled injections, respectively, during the experimental test activity. The reduced compression ratio of the engine provides the possibility of implementing late PCCI strategies at low loads to decrease NO_x emissions. At full load, the reduced compression ratio, coupled with a higher boost level, increases the low-end torque at the expense of some penalties pertaining to high-end torque [Catania *et al*., 2009].

The experimental campaign was carried out at the dynamic test bed of the Politecnico di Torino ICEAL (Internal Combustion Engines Advanced Laboratories), which is equipped with an 'ELIN AVL APA 100' cradle-mounted AC dynamometer. An 'AVL KMA 4000' fuel flowrate system was used to provide precise and continuous measurements of the engine fuel consumption, with a 0.1% accuracy over a 0.28-110 kg/h measuring range. The raw gaseous emissions from the engine were measured by means of an 'AVL AMAi60' system, made up of an analyzer train endowed with devices capable of simultaneously detecting gaseous concentrations of NO, NO_x, HC, CH_4, CO, CO_2 and O_2 chemical species. Another analyzer train was only equipped with a CO_2 instrument, which was mounted at the intake manifold to allow the EGR rate of the engine to be estimated [d'Ambrosio *et al.*, 2011]. Finally, an 'AVL 415S' smokemeter was used to evaluate the engine-out soot emissions.

The test engine was equipped with a high-frequency piezoelectric pressure transducer (Kistler 6058A), which was installed on the cylinder head to measure the in-cylinder temporal traces of the gas in cylinder #2. A high-frequency piezoresistive pressure transducer (Kistler 4005 BA), installed in the corresponding intake runner of the same cylinder, was used as a reference to obtain the absolute in-cylinder pressure measurement. Furthermore, pressure and temperature measurements were performed at different positions along the gas flow path (such as upstream and downstream of the turbocompressor, intercooler and turbine, in the intake manifold, in the runners and along the EGR circuit) by means of low-frequency piezoresistive pressure transducers and thermocouples.

All of the abovementioned measuring devices are controlled by AVL Puma Open 1.3.2 and IndiCom automation software. AVL CAMEO 3.8 was used to perform automatic tests related to the design of experiment (DoE). Data post-elaboration was conducted with the AVL CONCERTO 5 software.

3. EXPERIMENTAL TEST DESCRIPTION

The tested engine was provided by the OEM with a state-of-the-art pilot-main (*pM*) injection calibration, obtained without the utilization of statistical techniques. Starting from this calibration, triple and quadruple injection strategies, featuring pilot and/or after injections, were optimized by means of statistical Design of Experiment (DoE) procedures. The following engine operating points (expressed in terms of speed *n* [rpm] × *bmep* [bar]) were considered: 1500×2, 1500×5, 2000×2, 2000×5, 2500×8, 2750×12. These points were considered representative of the application of the engine to a vehicle over the New European Driving Cycle (NEDC). A variation list, made up of 120-150 tests, was obtained for each operating point by means of the MATLAB Model-Based Calibration toolbox, choosing a V-Optimal DoE [Montgomery, 2000]. After preliminary experimental analysis at the test bench, appropriate variation intervals and a suitable number of levels were chosen for the following engine parameters, considered as the most relevant input variables for the present investigation: start of the main injection (SOI_{Main}), dwell times between consecutive injection events (i.e., numbering the pilot injections as pilot 2 for the furthest from the main injection and pilot 1 for the closest, $DT_{Pil,2}$ between the pilot 2 and pilot 1 shots, $DT_{Pil,1}$ between pilot 1 and the main injections and DT_{Aft} between the main and after shots), injection quantities in each injection event ($q_{Pil,2}$, $q_{Pil,1}$ and q_{Aft}, while the fuel quantity q_{Main} pertaining to the main injection was not considered as an input parameter because it was set by the test bench control system in order to reach the desired *bmep* target value), intake air mass per stroke and per cylinder (m_{int}), rail pressure (p_{rail}), boost pressure (p_{int}, considered only at 2750×12, as it was found to have less influence on the combustion development at lower loads). Once a variation list for each engine operating point had been set up at the test bench, statistical quadratic models were built, as functions of the abovementioned input variables, for the following output variables: engine-out specific pollutant emissions (i.e., NO_x, soot, CO and HC), *bsfc* and CN. Each engine operating point was analyzed, by means of these statistical models, in order to obtain an optimal engine calibration. This calibration was based on several constraints on the selected output variables, which were set up on the basis of pollutant emission regulations, of the fuel economy requirements and of the after-treatment systems installed on the engine. Since this Euro 5 engine, in its passenger car layout, is equipped with a diesel oxidation catalyst (DOC) and a diesel particulate filter (DPF), and no specific after-treatment device is adopted as a countermeasure of NO_x emissions, the optimization criteria for all the injection strategies had the aim of minimizing NO_x, with respect to the

baseline pilot-main injection calibration provided by the OEM and implemented in the original ECU. At the same time, severe limits were set on CO, HC, *bsfc* and CN.

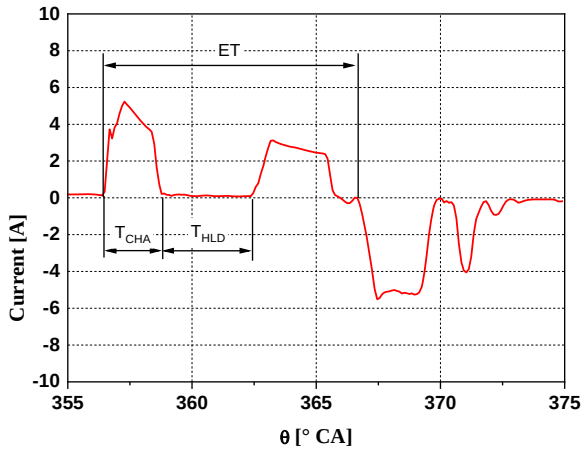

Figure 1. Boot injection parameters for an electrical current time history with DAP injectors.

Thanks to the installation of DAP injectors, it was possible to implement boot injection strategies. The DAP injector working principle allows a variable shaping of the injected fuel flow-rate to be obtained by means of a flexible modulation of the needle lift. A reduced charge of the piezo-stack during the early injection stage (for a T_{CHA} charging time duration) offers the possibility of keeping the needle in a partially open position over a T_{HLD} holding time interval (see Fig. 1 for a schematic representation of the T_{CHA} and T_{HLD} times). In such a way, the boot injection event is obtained. A second positive charging current is then given to the piezo-stack, and this allows the needle to reach its stroke-end and the injected fuel mass flowrate to reach its maximum value.

Different calibrations featuring boot injections were tested, starting from the DoE optimized multiple injections with the DAP injectors and replacing pilot 1 with a boot injection in order to obtain a boot-main (*bM*) injection event. Five different levels of T_{CHA} and four of T_{HLD} were implemented: T_{CHA} = 150, 160, 170, 180, 200 µs and T_{HLD} = 200, 300, 400, 500 µs. Moreover, they were combined to obtain a full factorial test plan (20 different combinations) for the boot injection strategy for each engine operating point. The dwell-time values between the *bM* injection and the other pilot and/or after shots were maintained to the values present in the original DoE optimized injection schedule, while the SOI referring to the *bM* injection was adjusted in order to have almost the same value of MFB50 (within a 1° CA variation band), regardless of the particular values of T_{CHA} and T_{HLD}. Furthermore, the inducted air mass, swirl actuator position, rail pressure and pilot/after injection quantities were also kept constant and equal to the corresponding DoE optimized calibration.

A comparison between the baseline *pM* double injection pattern, the DoE optimized triple injection calibrations (*ppM*, *pMa*) and the T_{CHA} and T_{HLD} full-factorial test plan for the boot injection strategies has been made in the next sections. The aim of this comparison has been to highlight the effects of the different strategies on engine-out pollutant emissions, *bsfc* and CN. At the lowest loads (referring to the abovementioned operating key points of the NEDC, in particular at 1500×2), the *pbM* boot injection strategy is compared with the baseline *pM* and with the DoE optimized *ppM*. At a medium-to-high load (i.e. at 2500×8), the boot strategies *bMa* and *pbMa* are compared with the baseline *pM* and with the DoE optimized *pMa*. At intermediate loads (i.e. at 2000×5), the comparison is performed between the boot *pbM* strategy, the baseline *pM* and the DoE optimized *pmM* (i.e., a pattern with double pilot injections, in which the pilot closest to the main shot, indicated as *m*, features a very short DT for which injection fusion occurs). Finally, EGR trade-offs are shown, at 1500×5, for all the triple and quadruple DoE optimized patterns and the baseline reference *pM* calibration.

In some cases (especially under the lowest speed/load conditions), not all the desired combinations of T_{CHA} and T_{HLD} values were implemented for the full factorial boot test plan, since some of them made it impossible to obain the desired injection pattern in combination with the desired engine load. For instance, if a particular boot calibration featured both a pilot and an after shot, with significant fixed amounts of fuel, the rest of the fuel quantity had to be injected during the *bM* injection event in order to match the desired *bmep* target. In this situation, if high T_{CHA} and T_{HLD} had to be set, the corresponding injected fuel q_{boot} was already sufficient during the boot phase to match the *bmep* target, thus making it unnecessary to open the injector needle any further at its stroke-end position and impossible to obtain a proper *bM* injection shot. In these cases, the corresponding T_{CHA} and T_{HLD} combinations for the boot injection were not tested.

Tables 2-12 report the main input values and other engine parameters (such as boost pressure, equivalence ratio and MFB50) of the calibration for both the baseline *pM* strategy and the triple and quadruple DoE optimized ones, and for each of the analyzed engine operating points.

4. BOOT VERSUS DOUBLE AND TRIPLE INJECTION STRATEGIES

Figures 2-8 report comparisons between the boot injection patterns and conventional double and triple injection strategies, in terms of engine-out pollutant emissions (NO_x, soot, HC and CO), *bsfc* and CN. Each figure shows the outcomes of a boot injection calibration

matrix test plan (obtained by varying the T_{CHA} and T_{HLD} values) together with those pertaining to the original pilot-main schedule (*pM*) and to the DoE optimized triple injection calibrations (*ppM*, at low loads or *pMa*, at the higher loads). Different symbols were used to distinguish each particular boot charging T_{CHA} value, while the x-axis scale reports the T_{HLD} boot duration values. Finally, the dashed lines represent the results of the baseline *pM* calibration provided by the OEM, while the solid lines refer to *ppM* or *pMa* strategies (obviously, as they do not feature any boot injection, no variation is shown with respect to either T_{CHA} or T_{HLD}).

4.1 Low load conditions (1500×2)

Figure 2 shows the NO_x and soot emissions for the pilot-boot-Main (*pbM*), the baseline *pM* and the DoE optimized *ppM* strategies, at 1500×2. A delayed fuel injection pattern timing was implemented, in addition to a large EGR fraction, for all the examined calibrations, to enable late PCCI conditions. By focusing on the boot strategy, it can be observed that engine-out NO_x emissions exhibit a slightly improving trend when the T_{CHA} values are reduced, while they seem to have a negligible dependence on T_{HLD}. The reduction in the T_{CHA} values, although leading to less injected fuel mass during the boot phase (q_{boot}), tends to further prolong the ID of the *bM* injection. In fact, the lower the T_{CHA} value is, the lower the injection pressure during the boot phase (due to the increased injector seat-needle fuel throttling) and, accordingly, the worse the mixing of the fuel droplets from the injectors with the inducted charge [Payri *et al*., 2013; d'Ambrosio and Ferrari, 2017c], thus making the ID of the *bM* injection become larger. Therefore, when the T_{CHA} values are reduced, a larger amount of fuel burns in the premixed phase (due to the augmented ID) and a diffusion combustion tail of lower intensity may be obserbed. It has already been demonstrated [d'Ambrosio and Ferrari, 2017a, 2017c] that variations in either T_{CHA} or T_{HLD}, in a late PCCI combustion mode, do not influence the maximum burned gas temperature ($T_{b,max}$) reached during the diffusion phase to any great extent. Nevertheless, since the diffusion combustion tail tends to be less relevant for lower T_{CHA}, the main combustion tends to be shorter during the expansion stroke, thus the exhaust gas temperatures T_{exh} deceases (in the examined case, if T_{CHA} decreases from 200 µs to 150 µs at a constant T_{HLD} = 200 µs, T_{exh} reduces from 285°C to 265°C). Therefore, recirculating exhaust gases at lower T_{exh} in the intake manifold also leads to slightly lower intake temperatures T_{int}. Since the inducted air mass is kept constant by the ECU at fixed engine points, in terms of *n* and *bmep*, the higher density EGR mass resulting from the lower T_{int} mixes with the fresh air and produces higher EGR rates (X_{EGR}) and reduced NO_x emissions [d'Ambrosio and Ferrari, 2015a].

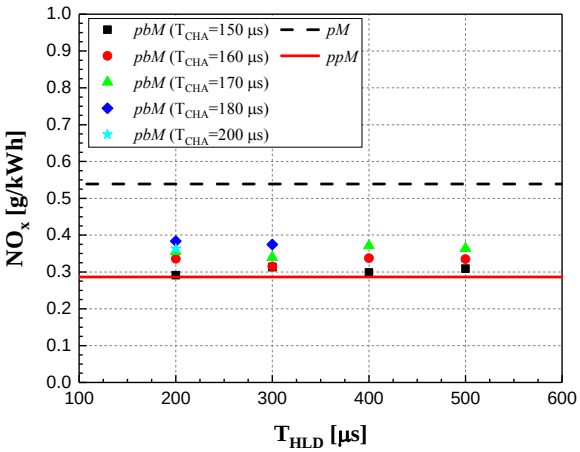

(a) NOx

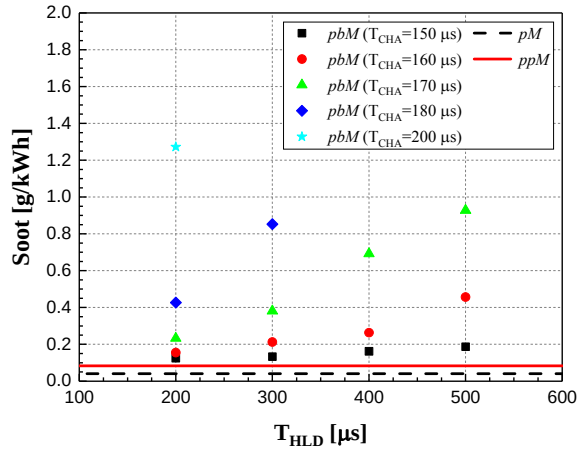

(b) Soot

Figure 2. NO_x (a) and soot (b) engine-out emissions for the *pbM*, *pM* and *ppM* injection strategies, at 1500×2.

When lower T_{CHA} values are implemented, the *pbM* strategy almost reaches the engine-out NO_x levels of the DoE optimized *ppM* strategy, without any further improvement. Furthermore, the *ppM* strategy leads to an appreciable reduction in engine-out NO_x emissions, with respect to the baseline *pM* calibration (0.29 g/kWh versus 0.54 g/kWh, respectively), this being the primary goal of its DoE optimization. The early introduction of a pilot injection (namely pilot 2) during the compression stroke, in the *ppM* strategy, is able to reduce the ID of the subsequent injections (both pilot 1 and the main injections). On the one hand, this advances the instant at which the burned gas flame temperatures overcome the 1900-2000 K range [d'Ambrosio and Ferrari, 2015b], thus prolonging the residence time of the burned gas at this higher thermal exposure and promoting N_2 oxidation reactions. On the other hand, it also mitigates the

premixed combustion intensity, thus reducing the peak flame temperatures, in correspondence to the diffusion flames, and hindering the NO_x formation mechanisms. NO_x formation mechanisms are particularly sensitive to local charge temperatures, according to the well-known Kamimoto-Bae diagram [Kamimoto and Bae, 1988], but the local equivalence ratio (ϕ) conditions (i.e., the local oxygen availability to oxidize the N_2 molecules) also play an important role, as only smaller local ϕ values than 1.5 allow NO_x to be produced (the presence of two pilot shots increases the local equivalence ratio values during the main combustion). In the case of a *ppM* pattern, as can be seen by comparing Tables 2 and 3, the optimization procedure leads to higher X_{EGR} (52.9%) than in the case of the baseline *pM* strategy (49.6%) or in that of all the *pbM* sweep calibrations (ranging from 50.5% to 52%). The combination of all these effects leads to the best overall results, in terms of NO_x engine-out emissions for the double pilot injection pattern, with respect to all the other considered calibration proposals.

Table 2: The main parameters of the baseline *pM* calibration at the 1500×2 engine point

Quantity	Value
SOI_{Main} [°CA bTDC]	-2.4
q_{Pil} [mg/hub]	1.7
DT_{Pil} [µs]	1462
X_{EGR} [%]	49.6
p_{Rail}[bar]	460
Boost [bar]	0.96
Global ϕ [-]	0.55
MFB50 [°CA aTDC]	17

Table 3: The main parameters of the DoE optimized *ppM* calibration at the 1500×2 engine point

Quantity	Value
SOI_{Main} [°CA bTDC]	-3.0
q_{Pil2} [mg/hub]	2.5
DT_{Pil2} [µs]	1500
q_{Pil1} [mg/hub]	2
DT_{Pil1} [µs]	500
X_{EGR} [%]	52.9
p_{Rail}[bar]	520
Boost [bar]	0.93
Global ϕ [-]	0.61
MFB50 [°CA aTDC]	14.9

The engine-out NO_x and soot emission trends for the *pbM* strategy, as can be seen by comparing Fig. 2a and Fig. 2b, follow a similar trend as T_{CHA} is varied, while a more evident increasing trend is clear for soot emissions than for NO_x emissions as T_{HLD} grows. This evidence highlights the absence of the usual NO_x-soot trade-off behavior, in line with the implementation of a late PCCI-like combustion mode. The reduction in T_{CHA}, which is beneficial for an NO_x emission reduction, has an even more pronounced effect on soot: the already explained increase in ID and the ensuing more relevant impact of the premixed combustion of the *bM* injection as T_{CHA} decreases, leads to the local formation of a more homogeneous mixture, which hinders the soot generation mechanisms. Furthermore, the relevant increasing trend as the T_{HLD} values grow, especially when the highest T_{CHA} values are implemented (i.e., $T_{CHA} \geq 170$ µs), could be due to interference phenomena between the injected fuel plumes during the *bM* injection event and the burned gases of the pilot injection. In fact, part of the fuel injected during the *bM* shot has to burn in an oxygen-poorer environment in which pilot combustion has just occurred (the pilot volume is relatively high, i.e. 2.5 mm^3, and its combustion tends to be separated from the subsequent *bM* one), and this promotes soot formation mechanisms. This is especially true for the highest values of T_{CHA} and T_{HLD}, which feature the largest q_{boot} injected quantity and, as already explained, the shortest ID (so that the combustion of the *bM* injected fuel is closer to the end of the pilot combustion). However, compared to the multiple injection strategies (*pM* and *ppM*), obvious detrimental effects on soot emissions are evident for any boot calibration, except for the lowest T_{CHA} and T_{HLD} combination. Although the baseline *pM* calibration shows nearly zero mass soot emissions, thanks to the implementation of the late PCCI-like strategy, slightly higher values (around 0.1 g/kWh) are observable in the case of a triple *ppM* injection strategy, even if they are too low to be considered as a cause of real concern. Apart from the consideration on the higher X_{EGR}, this may also be explained by considering the already discussed diminution of ID in the *ppM* strategy. The implementation of an additional pilot injection (pilot 2), coupled with the highest EGR rate strategy, leads to the formation of an increased number of locally rich mixture pockets (which are able to produce soot precursors) than in the case of a *pM* baseline injection pattern.

CN can be significantly influenced by changing the T_{CHA} or T_{HLD} boot parameters of the *pbM* strategy. As already mentioned, the ID, determined by the boot injection parameters, affects the premixed combustion intensity and, thus, the slope of the in-cylinder pressure rise. A close correlation exists between CN and the premixed combustion phase, which is generally responsible for the steepest increase in the in-cylinder pressure during combustion. Any countermeasure taken to limit the amount of fuel that burns under premixed combustion, such as increasing either the T_{CHA} or T_{HLD} values, is able to achieve CN improvements. Unfortunately, this behaviour, which is mainly related to the ID reduction of the *bM* injection, is the opposite of that of the soot emissions, thus an appreciable CN-soot trade-off is established (visible in Fig. 3b) for this low load condition. When boot injections are applied, CN

increases, compared with the multiple injection strategies. Both the *pM* and *ppM* strategies, represented by the dashed and the solid horizontal lines in Fig. 3a, respectively, show similar CN values, with a lower value for the *ppM* strategy.

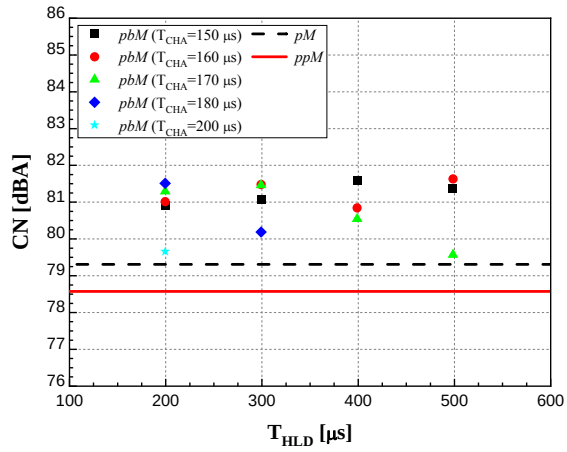

(a) CN

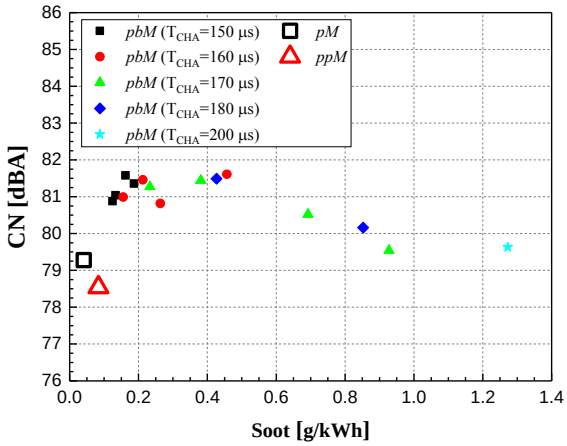

(b) Soot/CN trade-off

Figure 3. CN (a) and soot/CN trade-off (b) for the *pbM*, *pM* and *ppM* injection strategies, at 1500×2.

In this case, the result of such a remarkable beneficial effect on CN, which is achievable by introducing a second pilot shot into the injection pattern, as pointed out in several literature references, especially for low speeds and low loads [Maiboom *et al.*, 2008; Busch *et al.*, 2015a; Suk, 2014], is not evident. One of the reasons for this is that the DoE optimization procedure adopted for the *ppM* calibration was primarily set to optimize exhaust pollutant emissions rather than CN. Moreover, if the main combustion parameters of the *pM* and *ppM* injection strategies (Tables 2-3) are compared, *pM* is characterized by a more delayed combustion process (the fuel mass injected during the late main shot is higher in the *pM* injection pattern, which does not exploit a second pilot injection for fuel delivery).

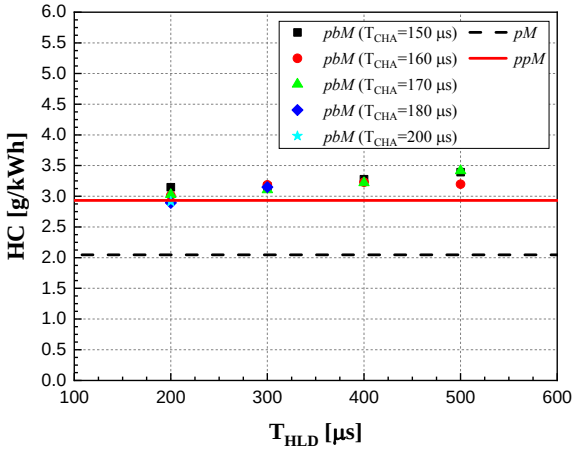

(a) HC

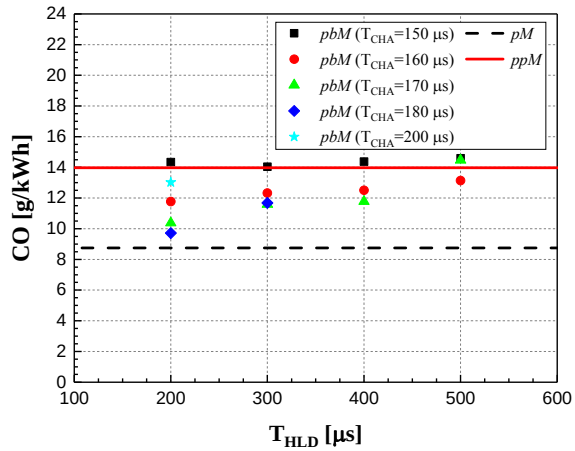

(b) CO

Figure 4. Engine-out HC (a) and CO (b) emissions for the *pbM*, *pM* and *ppM* injection strategies, at 1500×2.

The combustion process develops well during the expansion stroke, and this somewhat decreases the in-cylinder pressure derivative traces that are closely linked to the CN values (with more delayed values of MFB50 than the ppM strategy, that is, 16.7 °CA aTDC vs. 14.9 °CA aTDC). As a consequence, the *pM* strategy approaches the CN levels of the best double pilot case, even though slight penalties have been verified on *bsfc* for the former injection schedule [d'Ambrosio and Ferrari, 2015b].

The two plots depicted in Fig. 4 report the brake specific engine-out HC (Fig. 4a) and CO (Fig. 4b) emissions for the same previously considered calibrations. The high EGR mass recirculated and delayed injection pattern implemented at the considered low speed and load condition, together with the low compression ratio featured by the engine, are mainly

responsible for the high values of the CO and HC species. Regardless of the specific fuel injection pattern, a late PCCI-like combustion strategy leads to significantly lower combustion temperatures than a conventional diesel combustion mode. In addition, fuel over-mixing and flame quenching phenomena occur, which result be the main mechanisms responsible for unburned HC and CO at this low speed and low load condition, together with possible wall wetting phenomenon [Kiplimo *et al.,* 2012]. As far as the *pbM* strategy is concerned, the HC engine-out emissions, plotted in Fig. 4a, show very little dependence on either T_{HLD} or T_{CHA}. On the one hand, if T_{HLD} grows at a fixed T_{CHA}, as the injection train is advanced to maintain almost the same MFB50 value, over-mixing phenomena are promoted, which in turn increase the HC emissions. On the other hand, the same increase in T_{HLD} causes a reduction in the premixed phase of the *bM* combustion, and partly balances the effect of the over-mixing phenomena on HC. Moreover, the CO engine-out emissions do not show monotonic trends as T_{CHA} changes monotonically for the same boot strategy, while they tend to increase when T_{HLD} grows, especially for the highest T_{CHA} values (i.e., $T_{CHA} \geq 170$ μs). In fact, the higher T_{CHA} is, the larger the diffusion combustion tail, and this prolongs the duration of the main combustion during the expansion stroke with an ensuing increase in the exhaust gas temperatures, T_{exh}, which promote the final oxidation of CO into CO_2 [Kook *et al.*, 2005]. However, an increase in the T_{CHA} values tends to slightly decrease the maximum in-cylinder mean temperature during combustion [d'Ambrosio and Ferrari, 2017a], due to the reduced premixed phase. As CO emissions are particularly sensitive to this parameter, which does not take on high values at 1500×2, this can lead to a higher CO production rate during combustion. The balancing of the higher CO production rate (due to a lower maximum of the mean temperature in the cylinder) and the higher oxidation rate to CO_2 (due to a higher T_{exh}) when T_{CHA} increases, is probably the cause of the initial diminution (for instance, passing from T_{CHA}=150 μs to T_{CHA}=180 μs, at constant T_{HLD}=200 μs) and of the following growth in CO emissions (passing from T_{CHA}=180 μs to T_{CHA}=200 μs).

If the results of all the *pbM* calibrations are compared with the baseline *pM* and the optimized *ppM* ones, it can be observed that the engine-out CO and HC emissions of the boot strategies are roughly in line with those of the *ppM* strategy, while the *pM* calibration leads to the best results. On the one hand, if either a second pilot injection or a boot phase is introduced prior to the main shot, ID reduces. This in turn induces a faster ignition of the main injection and a consequent lower premixed main combustion phase, which likely reduces the occurrence of fuel overmixing of the main injection. On the other hand, the *ppM* strategy has been optimized through a DoE procedure, which resulted in a richer equivalence ratio than the double injection baseline pattern ($\phi = 0.61$ for *ppM* versus $\phi = 0.54$ for *pM*, see Tables 2-3). Both the *ppM* and *pbM* strategies (it should be recalled that the latter is derived directly from *ppM* by replacing the pilot event closest to the main shot with a boot phase, thus maintaining the same EGR fraction) feature a higher EGR rate than the baseline *pM* calibration, thereby counteracting the advantage of the reduced main ID. Furthermore, both *ppM* and *pbM* are set up with an early pilot 2 event that features a relatively large injection quantity (i.e., 2.5 mg/stroke, equal to around 25-30% of the total injected quantity over the cycle). The coupling of the advanced timing and a significant fuel quantity makes this pilot shot more prone to the occurrence of wall wetting phenomena, and possibly contributes to the total HC emissions of both the *ppM* and *pbM* strategies.

4.2 Medium-to-high load conditions (2500×8)

Tests to obtain a better understanding of the possible benefits achievable by the introduction of an after injection were only carried out at medium-to-high load conditions; this is in accordance to certain literature results that have defined an *imep* window starting from about 4 bar, where the after injection can be useful [Desantes *et al.*, 2007, O'Connor and Musculus, 2014a].

Comparisons were carried out between the baseline *pM* strategy, a DoE optimized calibration featuring a *pMa* triple injection strategy and two different boot injection calibrations featuring an after shot, either with (pilot-boot-Main-after, *pbMa*) or without (boot-Main-after, *bMa*) a pilot injection prior to the *bM* shot for the 2500×8 key point. The CO and HC emissions are not reported here, since they are not of great concern for this engine load.

The engine-out NO_x emissions in Fig. 5 do not show any appreciable sensitivity to variations of T_{CHA} or T_{HLD} for either the *bMa* or *pbMa* boot calibrations, in line with what is depicted for the 1500×2 engine operating point. The engine-out NO_x emission levels are higher than in the *bmep* = 2 bar case, due to the higher in-cylinder temperatures during the more vigorous diffusion combustion phase. The baseline *pM* calibration provides the worst results, with a NO_x emission level that is nearly double that of all the other strategies. It is worth recalling that the *pMa* strategy was optimized through a DoE procedure, with the main aim of reducing NO_x emissions, and that the boot injection calibrations were derived from the optimized *pMa* strategy.

By comparing the baseline *pM* with the *pMa* calibration parameters (see Tables 4-5), it emerges that a higher rail pressure and a lower EGR rate are implemented in the *pM* case: both these variations tend to create a shorter and closer to TDC combustion event. This increases the maximum temperature of the burned

gases and promotes NO_x formation. The delayed after injection, whose quantity is about 10% of the total injected quantity for all the examined injection patterns (*pMa*, *bMa* and *pbMa*), practically does not contribute to the NO_x emissions, as it burns in a relatively low-temperature environment during the expansion stroke.

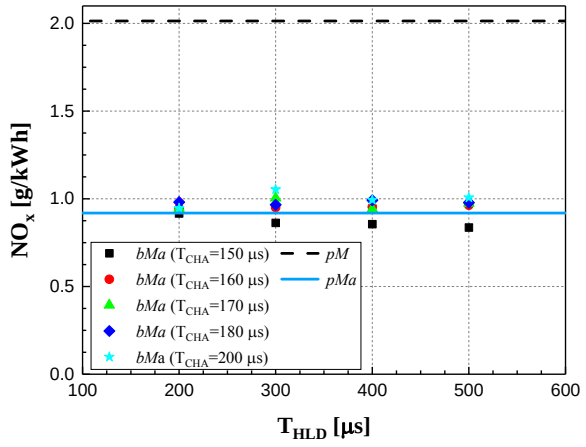

(a) *bMa*

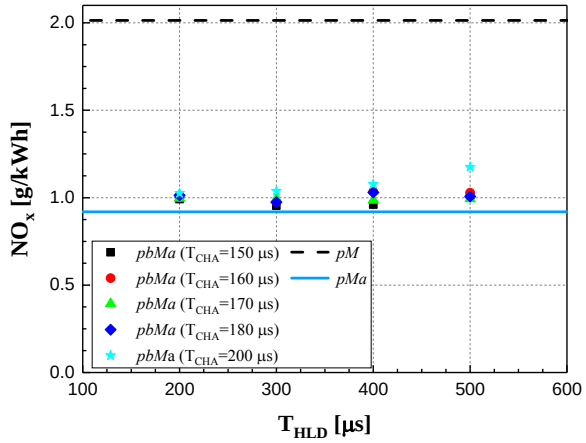

(b) *pbMa*

Figure 5. Engine-out NO_x emissions for the *bMa* (a), *pbMa* (b), *pM* and *pMa* injection strategies, at 2500×8.

Table 4: The main parameters of the baseline *pM* calibration at the 2500×8 engine point

Quantity	Value
SOI_{Main} [°CA bTDC]	2.7
q_{Pil} [mg/hub]	1.2
DT_{Pil} [µs]	1500
X_{EGR} [%]	25.1
p_{Rail}[bar]	1190
Boost [bar]	1.97
Global ϕ [-]	0.56
MFB50 [°CA aTDC]	15.4

Table 5: The main parameters of the DoE optimized *pMa* calibration at the 2500×8 engine point

Quantity	Value
SOI_{Main} [°CA bTDC]	2.5
q_{Pil} [mg/hub]	0.7
DT_{Pil} [µs]	740
q_{Aft} [mg/hub]	2.7
DT_{Aft} [µs]	1370
X_{EGR} [%]	27.2
p_{Rail}[bar]	1160
Boost [bar]	1.93
Global ϕ [-]	0.66
MFB50 [°CA aTDC]	19

The baseline *pM* strategy in Fig. 6 shows lower engine-out soot emissions. This result, together with what is shown in Fig. 5, highlights a clear NO_x-soot trade-off behavior, which is due to the presence of a conventional diesel combustion mode at this engine operating point. In the DoE optimized *pMa* case, the DT adopted between the pilot and main injections (around 740 µs, whereas it is more than 1500 µs in the case of the *pM* strategy, cf. Tables 4-5) prevents the pilot combustion from being completed before SOI_{Main}. Hence, interference phenomena between the main injected fuel plumes and the pilot combustion flames are more likely to occur than in the case of the *pM* strategy, and this results in a detrimental effect on the engine-out soot emissions. The engine-out soot emissions at this engine load prove to be less sensitive to boot calibration parameters than in the *bmep* = 2 bar case, due to the lower EGR fraction and higher in-cylinder temperatures, which have the effect of accelerating combustion reaction rates and of reducing the rate-shaping influence on combustion development. In fact, changing either T_{CHA} or T_{HLD} produces variations in the soot emissions that are restricted to a narrower band (i.e. from 0.25 to 0.55 g/kWh) than for the previously illustrated lower engine loads. The worst results for both the *bMa* and *pbMa* strategies arise from a combination of the highest T_{CHA} and T_{HLD} values (as occurred at 1500x2): the T_{CHA} =200 µs value in fact leads to higher soot levels than the *pMa* pattern. An increase in the T_{HLD} values enlarges the temporal duration of the fuel injection event, and thus retards the end of combustion. This generally causes an increase in soot emissions [Desantes *et al.*, 2004a], mostly as a result of the freezing of the oxidation rate during the expansion stroke. In addition, a longer T_{HLD} reduces the mean injection pressure throughout the whole boot-main event, thus worsening the fuel atomization and further contributing to increasing soot [d'Ambrosio and Ferrari, 2017a].

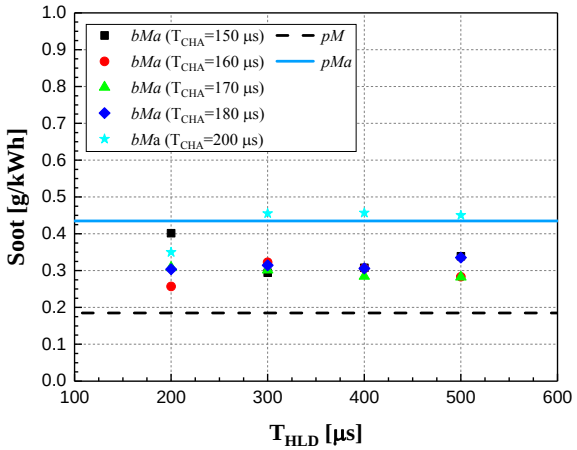

(a) *bMa*

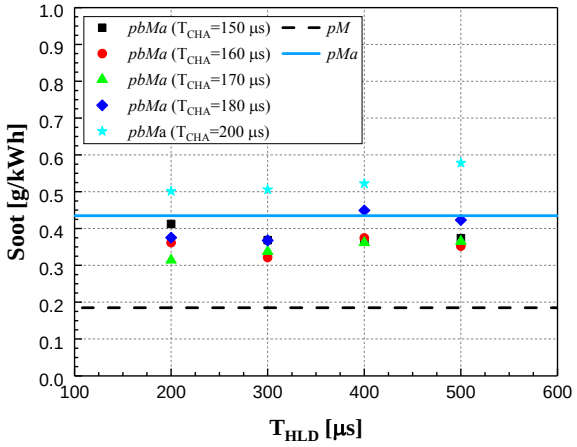

(b) *pbMa*

Figure 6. Engine-out soot emissions for the *bMa* (a), *pbMa* (b), *pM* and *pMa* injection strategies, at 2500×8.

Furthermore, an increase in the T_{CHA} value at a constant T_{HLD} seems to have two opposite effects, thus highlighting an inverting trend. Soot emissions tend to improve for the first increasing T_{CHA} steps (starting from T_{CHA} = 150 µs), while they generally become worse when the highest T_{CHA} values are reached (the maximum T_{CHA} is 200 µs). As already explained, increasing T_{CHA} leads to a diminution of the ID of the subsequent main injection, thus poorer mixing of the fuel with the intake charge and locally richer ϕ distributions can be expected, coherent with the higher soot formation rates. At the same time, increasing T_{CHA} increases the rail fuel pressure during the boot injection, thereby enhancing the fuel mixing with the intake charge and decreasing the soot formation rates.

The introduction of a delayed after injection, for all the examined *bMa*, *pbMa* and *pMa* strategies, does not help to achieve a notable reduction in engine-out soot emissions with respect to the baseline *pM* calibration. Different results can be found in the literature about the benefits of an after injection for the soot engine-out emissions at medium to high loads [Desantes *et al.*, 2007, O'Connor and Musculus, 2014a]. On the one hand, after shot combustion has the potential of interacting with the soot particles produced previously by the earlier injection events (the main and, possibly, pilot shots), and this leads to additional thermal energy that is in turn used to oxidize them [Desantes *et al.*, 2007]. On the other hand, if the after shot is too large, it can become detrimental for the engine-out soot emissions as it may produce more soot particles itself than the amount that it is able to oxidize. This can in part be caused by interference phenomena with the burned gas clouds generated by the previous injections, depending most of all on the swirl intensity and after injection timings [O'Connor and Musculus, 2014a]. In the present work, the after shot introduced at 2500×8 mainly has the potential of reducing NO_x: this is achieved by interrupting the late NO_x production due to the main shot; the further delayed after shot (DT_{Aft} = 1370 µs, i.e. a SOI_{Aft} of about 20 °CA aTDC, cf. Table 5), which burns at later instants during the expansion stroke, is less able to oxidize N_2 molecules and soot particles.

By comparing the two plots in Fig. 7, an improvement in CN can be observed as a result of introducing a pilot shot. As far as the *pbMa* calibration is concerned, the presence of a pilot injection mitigates the sensitivity of the CN to the boot injection parameters to a great extent; on the other hand, Fig. 7a highlights the significant negative impact of T_{CHA} and T_{HLD} on CN for the case of the *bMa* injection strategy. If the *bMa* calibration features the lowest values of both T_{CHA} and T_{HLD}, the highest CN is obtained, with an increase of about 3 dBA, compared to the conventional *pM* and *pMa* strategies or to the CN level pertaining to the *pbMa* calibration. This means that the application of a boot phase without a pilot shot (*bMa*) is not effective at a medium-to-high engine load.

All the calibrations featuring the after shot in Fig. 8 indicate a small *bsfc* variation, with the *pbMa* strategies showing the worst outcome. Splitting the injection event into multiple shots, together with the implementation of a boot injection, extends the combustion duration over a wider time interval, whereas a rapid burning near the TDC would maximize thermal efficiency.

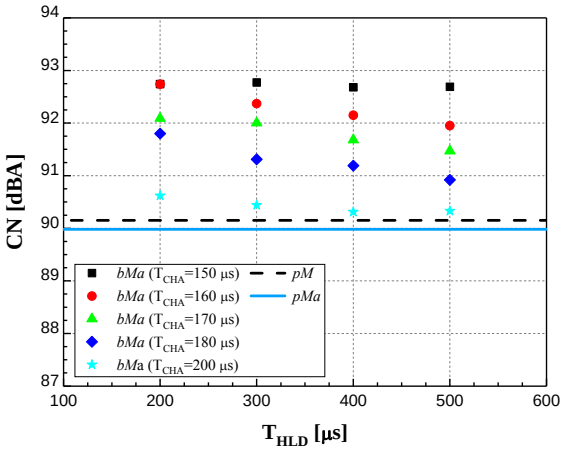

(a) *bMa*

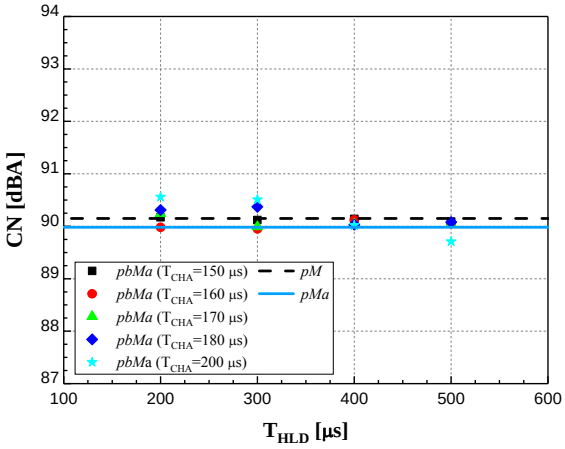

(b) *pbMa*

Figure 7. CN for the *bMa* (a), *pbMa* (b), *pM* and *pMa* injection strategies, at 2500×8.

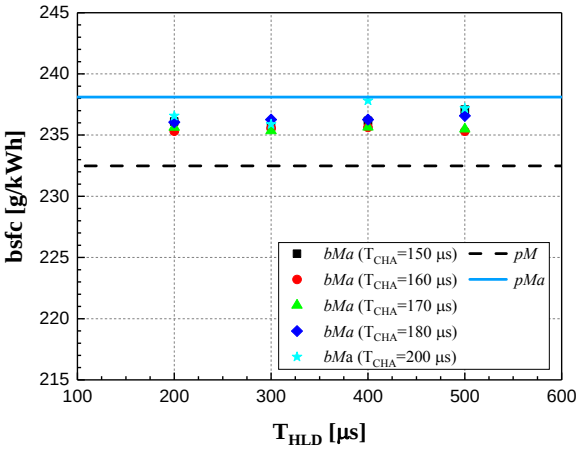

(a) *bMa*

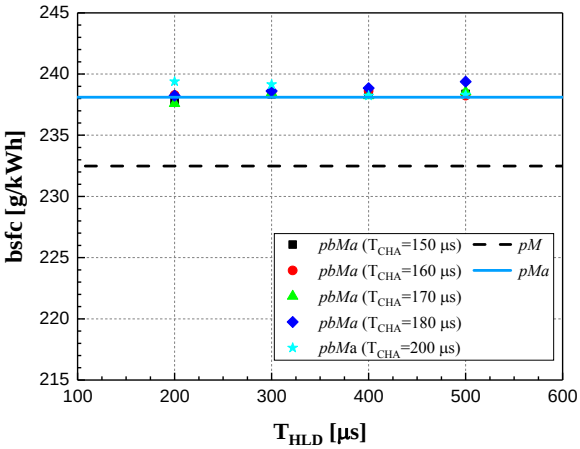

(b) *pbMa*

Figure 8. *bsfc* for the *bMa* (a), *pbMa* (b), *pM* and *pMa* injection strategies, at 2500×8.

Thus, the lowest fuel consumption (around 1.5% less than all the other solutions) is obtained for the conventional double *pM* injection. The earlier combustion of the *pM* strategy, with respect to the *pMa* one (MFB50 of 15.4 °CA aTDC, against 19 °CA aTDC for the *pMa* case, cf. Tables 4-5), together with the absence of a delayed after injection, results in a lower temperature at the engine exhaust (T_{exh}). This allows less thermal energy to be lost at the engine outlet, and explains the slight improvement in the *bsfc*. On the other hand, the higher T_{exh} pertaining to the after injection solutions could be exploited to reduce the turbocharger lag during engine transients [d'Ambrosio and Ferrari, 2015c].

5. BOOT VERSUS INJECTION FUSION STRATEGIES

All the previously discussed analyses have pointed out that each fuel injection event added to the main shot (i.e. pilot, boot and/or after injections) can have a significant and distinctive result on the final combustion characteristics, pollutant emissions and engine performance, due to its interaction with the mixture formation and its influence on combustion development. In this context, the application of a boot injection strategy did not allow a simultaneous improvement to be reached in all the considered engine outputs, although a good tendency to decrease NO_x emissions and CN was observed, but with an overall negative impact on soot emissions. The increased complexity of the DAP injection system, that was required to implement the boot phase, did not prove to be an attractive alternative

solution to more traditional fuel injection systems. Furthermore, if solenoid injectors are used, injection fusion phenomena could be exploited to obtain a similar continuous fuel rate-shaped injection to the boot injection achievable with the more expensive DAP injectors. Continuous rate-shaping can be obtained with the latest generation solenoid injectors by reducing the DT between closely-coupled pilot and main shots to values in the 120-140 µs range [Busch *et al.*, 2015a, 2015b; d'Ambrosio and Ferrari, 2017b]. This section presens a comparison between a double pilot injection strategy, featuring a pilot shot with a DT of around 120 µs (*pmM*, cf. Table 7), a *pbM* boot schedule with similar injection timing and the baseline *pM* calibration values (cf. Table 6) at medium load and the speed condition referring to the NEDC.

Table 6: The main parameters of the baseline *pM* calibration at the 2000×5 engine point

Quantity	Value
SOI_{Main} [°CA bTDC]	-1.2
q_{Pil} [mg/hub]	1.4
DT_{Pil} [µs]	1430
X_{EGR} [%]	34.6
p_{Rail}[bar]	750
Boost [bar]	1.35
Global ϕ [-]	0.60
MFB50 [°CA aTDC]	16.9

Table 7: The main parameters of the DoE optimized *pmM* calibration at the 2000×5 engine point

Quantity	Value
SOI_{Main} [°CA bTDC]	-0.6
q_{Pil2} [mg/hub]	1
DT_{Pil2} [µs]	1450
q_{Pil1} [mg/hub]	2.7
DT_{Pil1} [µs]	110
X_{EGR} [%]	41
p_{Rail}[bar]	720
Boost [bar]	1.32
Global ϕ [-]	0.64
MFB50 [°CA aTDC]	17.1

Figure 9 shows both the NO_x (Fig. 9a) and soot (Fig. 9b) emissions for the *pbM*, the baseline *pM* and the *pmM* strategies, at 2000×5. The two rate-shaped schedules (i.e. *pbM* and *pmM*) exhibit a similar tendency to improve NO_x emissions, compared to the baseline *pM* calibration, and *pbM* ensues penalties on soot emissions.

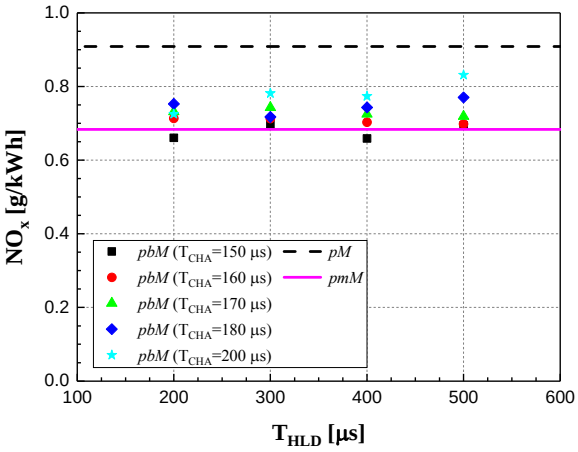

(a) NO_x

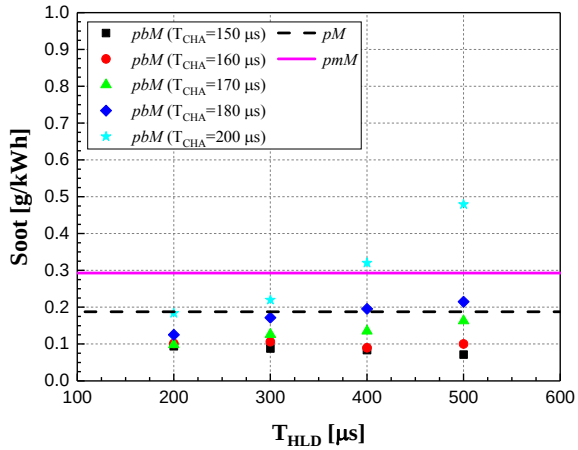

(b) Soot

Figure 9. NO_x (a) and soot engine-out (b) emissions for the *pbM*, *pM* and *pmM* injection strategies, at 2000×5.

This reduction in NO_x, of around 20%, may be ascribed to the use of a pilot shot prior to a rate-shaped main injection. Furthermore, the high EGR rates, the delayed injection timings and the low compression ratio all tend to decrease NO_x formation, thus masking the real potentiality of rate-shaping. Slight soot drawbacks can be observed for the application of either a pilot-main injection fusion or a boot phase prior to the main shot, if long T_{HLD} and T_{CHA} are implemented. The *pmM* strategy generally leads to better NO_x results and a worse soot performance than the *pbM* strategy, this result being in line with a conventional diesel combustion mode and the presence of a NO_x-soot trade-off.

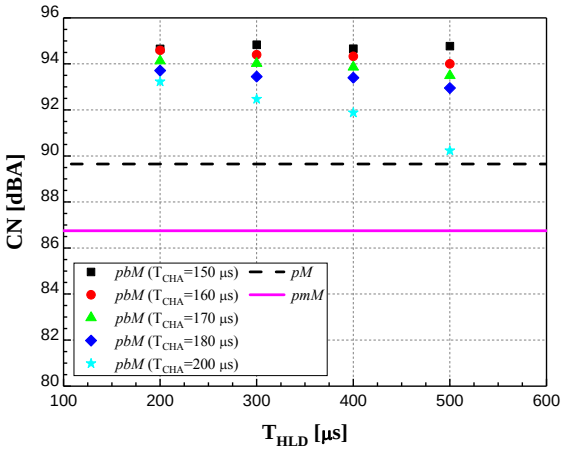

(a) CN

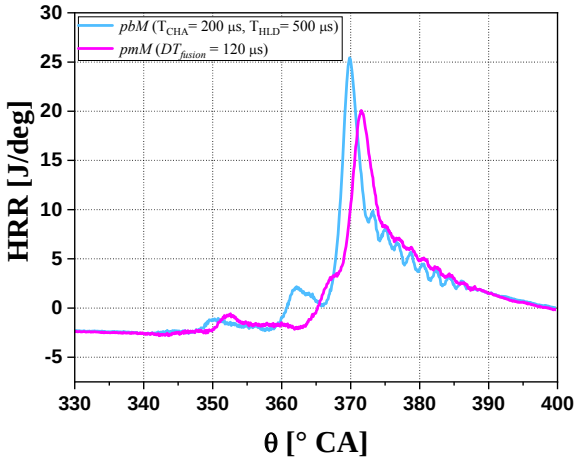

(b) HRR

Figure 10. CN for the *pbM*, *pM* and *pmM* (a) and HRR traces (b) for *pbM* (T_{CHA} = 200 µs and T_{HLD}=500 µ) and *pmM*, at 2000×5.

Interesting results have emerged from the CN analysis of the two examined fuel rate-shaping methods. The *pmM* fusion pattern exhibits the lowest CN level, while, among all the tested boot strategies, the schedule that implements the combination of the highest T_{CHA} and T_{HLD} values appears to be the best solution from the CN point of view. These two rate-shaped patternsimplement a similar pilot 2 event., i.e. nearly the same fuel injected quantity (q_{Pil2}), that is, about 1 mg/hub, and the same SOI_{Pil2}, about 20 °bTDC. Moreover, the SOI_{Pil1} of the fused pilot (*pmM*) is similar to the SOI of the boot phase in the *pbM* pattern and the equivalence ratio ϕ values are almost the same (around 0.65). Nevertheless, they exhibit a difference of about 3 dbA in the CN level (cf. Fig. 10a). As already explained, when boot strategies are applied, the prevailing noise reduction effect is related to the diminution of the ID of the main injection (this reduces the premixed formation). Instead, the noise reduction mechanism that prevails when the *pmM* strategy is applied is different. A distinctive, almost monotonic HRR signal (cf. the violet HRR trace in Fig. 10b, compared to the blue one pertaining to the *pbM* strategy featuring the best CN performance) is instead evident in the *pmM* case. As pointed out in [d'Ambrosio and Ferrari, 2017b], the evaporation of the main injected fuel, which is induced by pilot 1 combustion, smoothes the ongoing combustion process by absorbing heat. This reduces the HRR increase. This noise reduction mechanism is strong, and causes the *pmM* solution to be the most effective.

6. TRIPLE VERSUS QUADRUPLE INJECTION PATTERNS

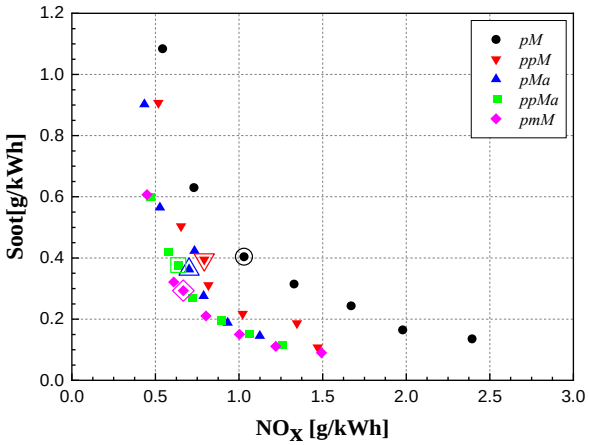

(a) NO_x-soot trade-off

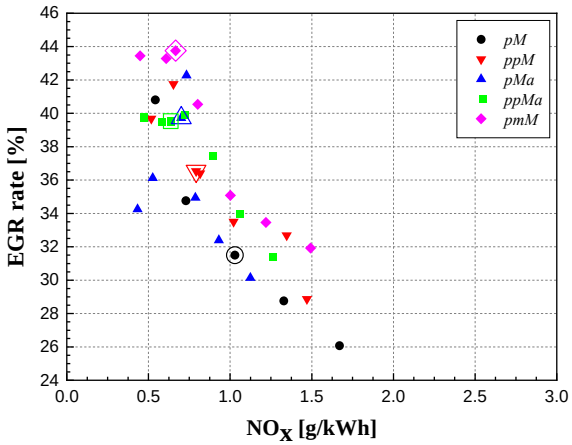

(b) EGR-NO_x trade-off

Figure 11. NO_x-soot trade-off (a) and EGR vs NO_x (b) for the *pM*, *ppM*, *pMa*, *ppMa* and *pmM* injection strategies, at 1500×5.

EGR trade-offs have been made at 1500x5, starting from the DoE optimized *ppM*, *pMa*, *pmM* and *ppMa*

calibrations (simultaneously featuring a double pilot and an after shot) and by varying the EGR rate of the baseline point (evidenced with a contoured symbol). Fig. 11a shows how all the triple and quadruple injection schedules (whose main baseline calibration parameters can be found in Tables 9-12) allow an appreciable improvement to be achieved in the NO_x-soot trade-off (a conventional diesel combustion mode takes place), with respect to the double baseline *pM* strategy (cf. Table 8). Soot can be reduced by splitting the injection pattern into more multiple shots than the double *pM* schedule, because the plumes of the sprays are not refilled with a continuous fuel flow-rate; in fact, a leaner charge is created each time an injection is cut off and then resumed [Reitz, 1998]. This soot reduction is possible if appropriate DTs are calibrated between the separate injection events, through the DoE optimization procedures. The soot reduction achievable by means of triple and quadruple injection patterns therefore allows the EGR fractions (Fig. 11b) to be increased with respect to the baseline *pM* calibration: this also contributes to reducing the NO_x emissions and justifies the improved NO_x-soot trade-off.

Table 8: The main parameters of the baseline *pM* calibration at the 1500×5 engine point

Quantity	Value
SOI_{Main} [°CA bTDC]	-2.4
q_{Pil} [mg/hub]	1.6
DT_{Pil} [µs]	1220
X_{EGR} [%]	31
p_{Rail}[bar]	590
Boost [bar]	1.16
Global ϕ [-]	0.64
MFB50 [°CA aTDC]	15

Table 9: The main parameters of the DoE optimized *ppM* calibration at the 1500×5 engine point

Quantity	Value
SOI_{Main} [°CA bTDC]	-1.5
q_{Pil2} [mg/hub]	0.85
DT_{Pil2} [µs]	600
q_{Pil1} [mg/hub]	2
DT_{Pil1} [µs]	950
X_{EGR} [%]	36.5
p_{Rail}[bar]	750
Boost [bar]	1.13
Global ϕ [-]	0.68
MFB50 [°CA aTDC]	13.8

Table 10: The main parameters of the DoE optimized *pMa* calibration at the 1500×5 engine point

Quantity	Value
SOI_{Main} [°CA bTDC]	-1.6
q_{Pil} [mg/hub]	1.9
DT_{Pil} [µs]	980
q_{Aft} [mg/hub]	1
DT_{Aft} [µs]	1130
X_{EGR} [%]	39.5
p_{Rail}[bar]	600
Boost [bar]	1.13
Global ϕ [-]	0.68
MFB50 [°CA aTDC]	14.2

Table 11: The main parameters of the DoE optimized *ppMa* calibration at the 1500×5 engine point

Quantity	Value
SOI_{Main} [°CA bTDC]	-1.7
q_{Pil2} [mg/hub]	0.8
DT_{Pil2} [µs]	600
q_{Pil1} [mg/hub]	1
DT_{Pil1} [µs]	900
q_{Aft} [mg/hub]	0.8
DT_{Aft} [µs]	680
X_{EGR} [%]	39.5
p_{Rail}[bar]	620
Boost [bar]	1.13
Global ϕ [-]	0.70
MFB50 [°CA aTDC]	15.6

Table 12: The main parameters of the DoE optimized *pmM* calibration at the 1500×5 engine point

Quantity	Value
SOI_{Main} [°CA bTDC]	-0.5
q_{Pil2} [mg/hub]	2
DT_{Pil2} [µs]	400
q_{Pil1} [mg/hub]	3
DT_{Pil1} [µs]	110
X_{EGR} [%]	43.7
p_{Rail}[bar]	770
Boost [bar]	1.12
Global ϕ [-]	0.70
MFB50 [°CA aTDC]	12

Figure 12 shows the CN values of all the examined triple and quadruple injection patterns and of the *pmM* schedule. In this case, the *pmM* strategy still shows a satisfactory performance, but does not result in the lowest absolute CN, which is instead achieved for the double pilot *ppM* calibration. The DoE optimization procedure (built with a similar CN constraint to that of all the other calibrations) was used to set up a *pmM* calibration that featured a more advanced SOI_{Main} than the other solutions, and therefore produced a more advanced MFB50. This

more advanced MFB50 makes the main combustion occur earlier during the expansion stroke, and with higher in-cylinder pressure first derivatives (with a peak of approximately 3 bar/°CA, located at 8 °CA aTDC, as can be seen in Fig. 12b) than for the triple and quadruple schedules. On the one hand, this negatively affects the CN level, but this is almost completely balanced by the suppressing noise interaction between the fused pilot and main combustion fields.

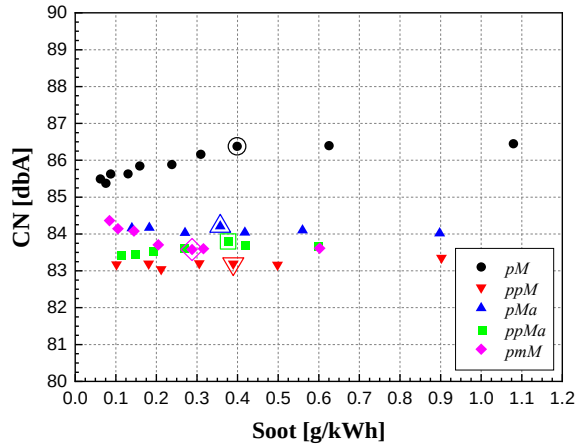

(a) CN vs soot

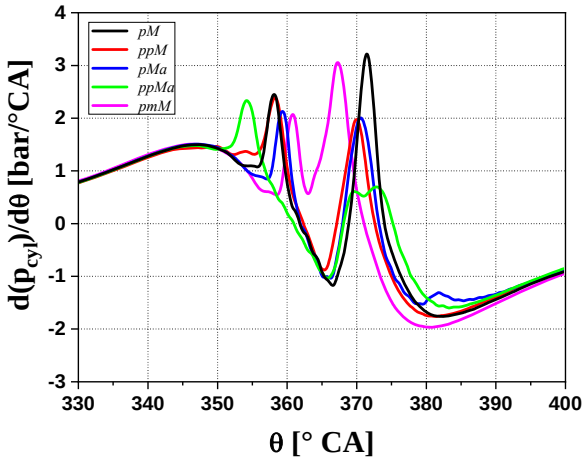

(b) In-cyl pressure first derivative

Figure 12. CN vs soot (a) and in-cylinder pressure first derivative (b) for the *pM*, *ppM*, *pMa*, *ppMa* and *pmM* injection strategies, at 1500×5.

On the other hand, as can be detected in Fig. 13, advancing the injection timing can lead to advantages in terms of bsfc as well as CO and HC engine-out emissions (which have not been reported here since they are not critical emissions for medium speeds and loads): the *pmM* combustion, closer to TDC, ensures better efficiency as well as enough time and thermal energy to prevent incomplete combustion from taking place and the oxidation of CO and HC to be induced.

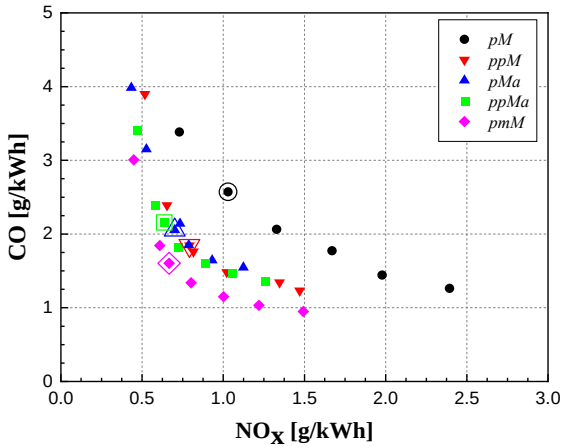

(a) CO

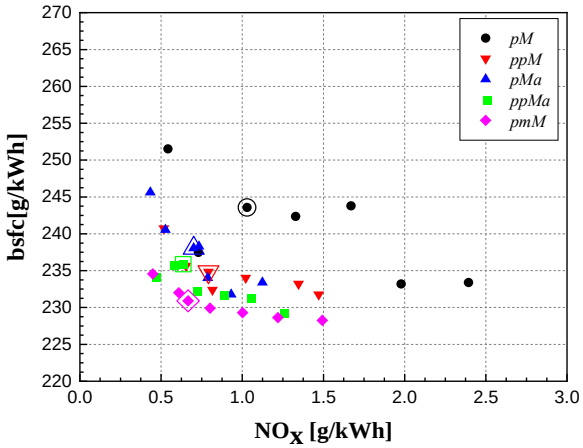

(b) bsfc

Figure 13. CO vs NO_x (a) and bsfc vs NO_x (b) for the *pM*, *ppM*, *pMa*, *ppMa* and *pmM* injection strategies, at 1500×5.

7. CONCLUSION

The potentialities of boot rate-shaped injections, multiple injection strategies and injection fusion schedules have been investigated. The experimental tests were performed in a low-compression ratio Euro 5 passenger car diesel engine, under low to medium speed and load operating conditions.

High rates of EGR, that is, higher than 50% for the lowest loads, in addition to delayed fuel injection patterns, have made it possible to reach late PCCI-like combustion modes at 1500×2. A notable reduction in NO_x emissions was thus made possible, due to the EGR dilution effect and the combustion development during the expansion stroke, both of which induce a reduction in the the peaks of the in-cylinder gas temperature. Certain drawbacks, such as deteriorated fuel consumption and increased

emission of the CO and HC species, generally emerged, due to the premixed combustion and the relatively low exhaust temperature. The effect of the boot injection parameters on NO_x emissions was relatively low in these low load PCCI-like conditions, compared to conventional diesel combustion modes: the NO_x reduction is mainly due to the EGR effects and to the delayed injection timings.

At *bmep* = 8 bar, DoE was used to optimize the *pMa* calibration and the calibrations derived from the boot strategies (*bMa* and *pbMa*), realized with the DAP injectors, which featured higher EGR rates, lower rail pressure and slightly more delayed injection timings than the baseline *pM* strategy, and thus nearly halved the NO_x emission level. The boot parameters had a significant influence on soot emissions. The worst soot emissions were obtained for the highest T_{CHA} and T_{HLD} values (up to 10 times the soot level of the reference *pM* calibration).

Introducing a second pilot injection (*ppM*) or a long T_{CHA} and T_{HLD} boot phase has proved to effectively mitigate the CN levels. Oddly, the *pMa* strategy, implemented at *bmep* = 8 bar also seemed to provide slight CN reductions, with respect to the baseline *pM* strategy, but this is only due to the indirect impact of the after injection on the DoE optimized pilot injection parameters.

Furthermore, conventional optimized triple and quadruple DoE injection strategies can lead to improved soot-NO_x trade-off behavior at medium loads and speeds.

Finally, if injection fusion strategies are implemented with solenoid injectors for medium loads and speeds, CN reductions of up to 3.5 dbA can be found, compared to the baseline *pM* strategy. In general, injection fusion strategies, achieved by means of solenoid injectors, seem to guarantee a better performance than boot injection strategies obtained by means of DAP injectors.

In short, the optimum engine calibrations for low and medium loads and speeds should feature triple or quadruple injections together with possible pilot-main fusion injection events.

The introduction of a delayed after injection at 2500×8, in a *pMa* schedule, did not help to reduce the soot penalties to any great extent, compared to the baseline *pM* calibration (the benefits of the after shot on the *CN* were only due to its impact on the DoE optizitation of the pilot injection); this also occured because the considered DoE optimization procedure had the primary goal of abating NO_x. As a result, the implemented after injection quantity and timing were more able to reduce the late NO_x production, by interrupting the main combustion, than to oxidize the previously formed soot particles.

ACKNOWLEDGEMENTS – AVL is acknowledged for having provided the CAMEO 3.8 and CONCERTO 5 licenses within the University Partnership Program

REFERENCES

Balaji, M., Wenming, Y., Siaw, K. C. (2013). Fuel injection strategies for performance improvement and emissions reduction in compression ignition engines - A review. *Renewable and Sustainable Energy Reviews* **28**, 664-676.

Busch, S., Zha, K., Miles, P. C. (2015). Investigations of closely coupled pilot and main injections as a means to reduce combustion noise in a small-bore direct injection Diesel engine. *International Journal of Engine Research* **16**, **1**, 13-22.

Busch, S., Zha, K., Warey, A., Pesce, F., Peterson, R. (2015). On the Reduction of Combustion Noise by a Close-Coupled Pilot Injection in a Small-Bore DI Diesel Engine. ASME Internal Combustion Engine Division Fall Technical Conference, Volume 2: Emissions Control Systems; Instrumentation, Controls, and Hybrids; Numerical Simulation; Engine Design and Mechanical Development, ICEF2015-1004, V002T06A003 1-18.

Catania A., Ferrari A., Mittica A. (2006). High-pressure rotary pump performance in multi-jet common rail systems. Proceedings of 8th Biennial ASME Conference on Engineering Systems Design and Analysis, ESDA2006. *Engineering Systems Design and Analysis, Volume 4: Fatigue and Fracture, Heat Transfer, Internal Combustion Engines, Manufacturing, and Technology and Society*, 557-565.

Catania A., Ferrari A., Mittica A., Spessa E. (2007). Common rail without accumulator: Development, theoretical-experimental analysis and performance enhancement at DI-HCCI level of a new generation FIS. *SAE Technical paper* 2007-01-1258.

Catania, A., d'Ambrosio, S., Finesso, R., Spessa, E., Cipolla, G., Vassallo, A. (2009). Combustion System Optimization of a Low Compression-Ratio PCCI Diesel Engine for Light-Duty Application. *SAE Int. J. of Engines* **2**, **1**, 1314-1326.

Catania, A., d'Ambrosio, S., Finesso, R., Spessa, E. (2010). Effects of Rail Pressure, Pilot Scheduling and EGR Rate on Combustion and Emissions in Conventional and PCCI Diesel Engines. *SAE Int. J. of Engines* **3**, **1**, 773-787.

d'Ambrosio, S., Ferrari, A. (2015). Effects of exhaust gas recirculation in diesel engines featuring late PCCI type combustion strategies. *Energy Conversion and Management* **105**, 1269-1280.

d'Ambrosio, S., Ferrari, A. (2015). Potential of double pilot injection strategies optimized with the design of experiments procedure to improve diesel engine emissions and performance. *Applied Energy* **155**, 918-932.

d'Ambrosio, S., Ferrari, A. (2015). Potential of Multiple Injection Strategies Implementing the After Shot and Optimized with the Design of Experiments Procedure to Improve Diesel Engine Emissions and Performance. *Applied Energy* **155**, **10**, 933-946.

d'Ambrosio, S., Ferrari, A. (2016). Effects of pilot injection parameters on low temperature combustion diesel engines equipped with solenoid injectors featuring conventional and rate-shaped main injection. *Energy Conversion and Management* **110**, 457-468.

d'Ambrosio, S., Ferrari, A. (2017). Boot injection dynamics and parametrical analysis of boot shaped injections in low-temperature combustion diesel engines for the optimization of pollutant emissions and combustion noise. *Energy* **134**, 420-437.

d'Ambrosio, S., Ferrari, A. (2017). Exploitation of injection fusion strategies in diesel engines equipped with solenoid injectors. *International Journal of Engine Research* **19**, **6**, 653-667.

d'Ambrosio, S., Ferrari, A. (2017). Potentialities of Boot Injection Combined with After Shot for the Optimization of Pollutant Emissions, Fuel Consumption and Combustion Noise in Passenger Car Diesel Engines. *SAE Int. J. of Engines* **10, 2**, 144-159.

d'Ambrosio, S., Finesso, R, Spessa, E. (2011). Calculation of mass emissions, oxygen mass fraction and thermal capacity of the inducted charge in SI and diesel engines from exhaust and intake gas analysis. *Fuel* **90**, **1**, 152-166.

d'Ambrosio, S., Gaia, F., Iemmolo, D., Mancarella, A. *et al.* (2018). Performance and Emission Comparison between a Conventional Euro VI Diesel Engine and an Optimized PCCI Version and Effect of EGR Cooler Fouling on PCCI Combustion. *SAE Technical Paper* 2018-01-0221.

Desantes, J. M., Arrègle, J., Lopez, J. J., Garcia, A. (2007). A comprehensive study of diesel combustion and emissions with post injection. *SAE Technical Paper* 2007-01-0915.

Desantes, J. M., Benajes, J., Molina, S., Gonzales, C. A. (2004). The modification of the fuel injection rate in heavy-duty diesel engines. Part 1: effects on engine performance and emissions. *Applied Thermal Engineering* **24**, **17-18**, 2701-2714.

Desantes, J. M., Benajes, J., Molina, S., Gonzalez, C. A. (2004). The modification of the fuel injection rate in heavy-duty diesel engines Part 2: Effects on combustion. *Applied Thermal Engineering* **24, 17-18**, 2715-2726.

Ehleskog, R., Ochoterena, R. L., Andersson, S. (2007). Effects of multiple injections on engine-out emission levels including particulate mass from an HSDI diesel engine. *SAE Technical Paper* 2007-01-0910.

Fang, Q., Fang, J., Zhuang, J., Huang, Z. (2012) Influences of pilot injection and exhaust gas recirculation (EGR) on combustion and emissions in a HCCI-DI combustion engine. *Applied Thermal Engineering* **48**. 97-104.

Ferrari, A., Mittica, A. (2012). FEM modeling of the piezoelectric driving system in the design of direct-acting diesel injectors. *Applied Energy* **99**, 471-483.

Ferrari, A., Mittica, A. (2016). Response of different injector typologies to dwell time variations and a hydraulic analysis of closely coupled and continuous rate shaping injection schedules. *Applied Energy* **169**, 899-911.

Ferrari, A., Mittica, A., Paolicelli, F., Pizzo, P. (2016). Hydraulic Characterization of Solenoid-actuated Injectors for Diesel Engine Common Rail Systems. *Energy Procedia* **101**, 878-885.

Ferrari, A., Mittica, A., Pizzo, P., Jin, Z. (2018). PID Controller Modelling and Optimization in CR Systems with Standard and Reduced Accumulators. International Journal of Automotive Technology **19**, **5**, 771-781.

Ferrari, A., Mittica, A., Pizzo, P., Wu, X., Zhou, H. (2018). New methodology for the identification of the leakage paths and guidelines for the design of common rail injectors with reduced leakage. *Journal of Engineering for Gas Turbines and Power* **140**, **2**, 022801 1-10.

Ferrari, A., Mittica, A., Spessa, E. (2012). Benefits of hydraulic layout over driving system in piezo-injectors and proposal of a new-concept CR injector with an integrated Minirail. *Applied Energy* **103**, 243-255.

Finesso R, Hardy G, Mancarella A, Marello O, Mittica A, Spessa E (2019). Real-Time Simulation of Torque and Nitrogen Oxide Emissions in an 11.0 L Heavy-Duty Diesel Engine for Model-Based Combustion Control. *Energies* **12**, 460.

Helmantel, A., Golovitchev, V. (2009). Injection Strategy Optimization for a Light Duty DI Diesel Engine in Medium Load Conditions with High EGR rates. *SAE Technical Paper* 2009-01-1441.

Heywood, J. B. (2018). *Internal combustion engine fundamentals*. 2nd edn. McGraw Hill. New York.

Hoimyung, C., Jeongwoo, L., *et al.* (2013). Comparison of the effects of multiple injection strategy on the emissions between moderate and heavy EGR rate conditions: part 2-post injections. *J. of Mechanical Science and Technology* **27**, **7**, 2217-2223.

Kamimoto, T., Bae, M. (1988). High Combustion Temperature for the Reduction of Particulate in Diesel Engines. *SAE Technical Paper* 880423.

Kastner, O., Atzler, F., Juvenelle, C., Rotondi, R., Weigand, A. (2009). Directly actuated piezo injector for advanced injection strategies towards cleaner diesel engines. 7th international symposium towards clean diesel engines (TCDE), Aachen, 4-5 June 2009.

Kiplimo, R., Tomita, K. N., Yokobe, S. (2012). Effects of spray impingement, injection parameters, and EGR on the combustion and emission characteristics of a

PCCI diesel engine. *Applied Thermal Engineering* **37**, 165-175.

Kook, S., Bae, C., Miles, P., Choi, D. *et al*. (2005). The Influence of Charge Dilution and Injection Timing on Low-Temperature Diesel Combustion and Emissions. *SAE Technical Paper* 2005-01-3837.

Maiboom, A., Tauzia, X., Hetet, J. F. (2008). Experimental study of various effects of exhaust gas recirculation on combustion and emissions of an automotive direct injection diesel engine. *Energy* **33**, **1**, 22-34.

Montgomery, D. C. (2000). *Design and Analysis of Experiments*. 5th edn. Wiley. New York.

Musculus, M. P. B., Miles, P. C., Pickett, L. M. (2012). Conceptual models for partially premixed low-temperature diesel combustion. *Progress in Energy and Combustion Science* **39**, **2-3**, 246-283.

O'Connor, J., Musculus, M. P. B. (2014). Effect of load on close-coupled post-injection efficacy for soot reduction in an optical, heavy duty diesel research engine. *Journal of Engineering for Gas Turbines and Power* **136**, **10**, 101509 1-16.

O'Connor, J., Musculus, M. P. B. (2014). In-Cylinder Mechanisms of Soot Reduction by Close-Coupled Post-Injections as Revealed by Imaging of Soot Luminosity and Planar Laser-Induced Soot Incandescence in a Heavy-Duty Diesel Engine. *SAE Int. J. of Engines* **7**, **2**, 673-693.

Okude, K., Mori, K., Shiino, S. *et al*. (2007). Effects of Multiple Injections on Diesel Emission and Combustion Characteristics. *SAE Technical Paper* 2007-01-4178.

Payri, R., Gimeno, J., Bardi, M., Plazas, A. H. (2013). Study Liquid Length Penetration Results Obtained with a Direct Acting Piezo Electric Injector. *Applied Energy* **106**, **6**, 152-162.

Reitz, R. D. (1998). Controlling D.I. Diesel Engine Emissions Using Multiple Injections and EGR. *Combustion Science and Technology* **138**, **1-6**, 257-278.

Reşitoğlu, İ., Altinisik, K., Keskin, A. (2014). The pollutant emissions from diesel-engine vehicles and exhaust aftertreatment systems. *Clean Technologies and Environmental Policy* **17**, **1**, 15-27.

Suh, K. H. (2014). Study on the twin-pilot-injection strategies for the reduction of the exhaust emissions in a low-compression engine. *Proceedings of the I. of Mech. Engineers, Part D: J. of Automobile Eng.* **228**, **3**, 335-343.